

# Copper Oxide Doped Carbon Catalyst for Anodic Half-Cell of Vanadium Redox Flow Battery

Irshad U. Khan, Tanmay Paul, Murali Mohan Seepana

**Abstract**—This paper presents a study on synthesizing and characterizing a Copper Oxide Doped Carbon (CuO-C) electrocatalyst for the negative half-cell reactions of Vanadium Redox Flow Battery (VRFB). The CuO was synthesized using a microreactor. The electrocatalyst was characterized using X-ray Diffraction (XRD), Fourier Transform Infrared Spectroscopy (FTIR), and Field Emission Scanning Electron Microscopy (SEM). The electrochemical performance was assessed by Linear Sweep Voltammetry (LSV). The findings suggest that the synthesized CuO exhibited favorable crystallinity, morphology, and surface area, leading to improved cell performance.

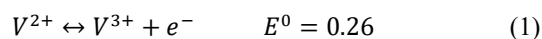
**Keywords**—ECSA, electrocatalyst, energy storage, Tafel.

## I. INTRODUCTION

VANADIUM redox flow batteries (VRFBs) have emerged as a prominent technology for large-scale energy storage due to their scalability and flexibility in providing energy storage solutions [1]. Electrodes are critical components of VRFBs that play a crucial role in the electrochemical reactions that occur during the battery's operation. The anode is responsible for oxidizing the vanadium ions in the anolyte, while the cathode reduces the vanadium ions in the catholyte. The efficiency of the anode reaction is dependent on the electrocatalyst used to facilitate the reaction (1) [2]. To enhance the electrochemical performance of VRFBs, the development of high-performance anode materials has been an active area of research.

CuO is an abundant and cost-effective material that exhibits excellent electrocatalytic activity. In this work, the focus is on the synthesis of CuO using microreactor to develop electrocatalyst for VRFB and its characterization using various techniques such as XRD, FTIR, and SEM.

We also investigate the electrochemical performance of CuO-C as an anode material in VRFBs, including LSV and Tafel analysis. The present study provides valuable insights into using CuO-C as an efficient anode side catalyst for VRFBs and developing highly active and economic electrocatalysts for energy storage applications.



## II. EXPERIMENTAL

### A. Materials

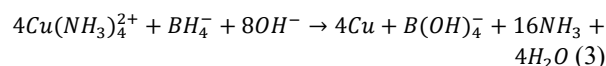
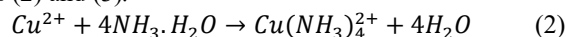
All chemicals used in the experiment are analytic reagent

Irshad U Khan and Tanmay Paul are with the National Institute of Technology, Warangal, 506004 India (e-mail: irshad@student.nitw.ac.in, tpch21104@student.nitw.ac.in).

grade. Copper acetate monohydrate  $Cu(CH_3COO)2H_2O$  and acetic acid glacial were purchased from Merck, India. Sodium hydroxide NaOH (pellets) was purchased from Lobha Chemie.  $H_2SO_4$  was procured from Finar India Ltd. Vanadium (IV) oxide sulfate hydrate ( $VOSO_4$ ) purchased from Himedia. Deionized water was used throughout the experiment.

### B. Synthesis of CuO

CuO particles were synthesized by using the micro-reactor [3]. A solution of  $CuSO_4$  (0.2 mol/L) and a solution of  $NaBH_4$  (0.4 mol/L) were prepared. The slow addition of ammonium hydroxide solution caused the blue color of the  $CuSO_4$  solution to change to dark blue. Both solutions were adjusted to a pH range of 10-12 by mixing NaOH solution. To act as dispersing agents, polyvinylpyrrolidone (PVP, MW 360,000) solution (3.2 g/L) was added to the  $CuSO_4$  solution.  $CuSO_4$  and  $NaBH_4$ , were pumped into the stainless steel microreactor continuously as shown in Fig. 1 and following the reaction scheme proposed in reactions (2) and (3).



### C. Preparation of Electrocatalyst

The IPA and water in the ratio of 1:1 were mixed homogeneously using a stirrer for 10 min. The powdered carbon, CuO, and Nafion solution were added to the above solution and ultrasonicated for 30 min to obtain the electrochemical sol (CuO-C). The homogeneous sol is layered on Carbon Paper (CP) followed by drying at room temperature for 12 h.

### D. Characterization

Surface micromorphology of the synthesized CuO-C electrocatalyst coated on pristine carbon substrate was observed using FESEM (model: Ultra 55 Make: ZEISS) and comparison with bare carbon paper is reported. The CuO-C electrocatalyst was coated over a glass slide and kept for drying. The layer was peeled and made a powdered sample for XRD and FTIR characterization.

The powder sample was analyzed by X-ray diffractometer (Make: PANalytical & model: X'Pert Powder). The dried powdered sample was mixed with KBr and pressed to make a pellet and mounted into the sample holder of FTIR spectrometer (make: PerkinElmer Spectrum, model: 100S) and analyzed for

Murali Mohan Seepana\* is with the National Institute of Technology, Warangal, 506004 India (corresponding author, phone: 0870-2462630; e-mail: murali@nitw.ac.in).

the presence of respective functional bonds.

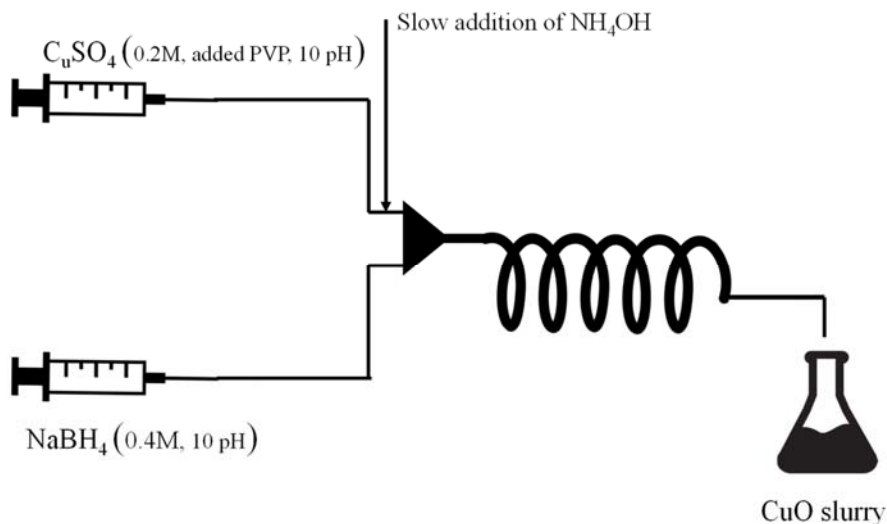


Fig. 1 Schematic diagram of synthesis procedure of CuO

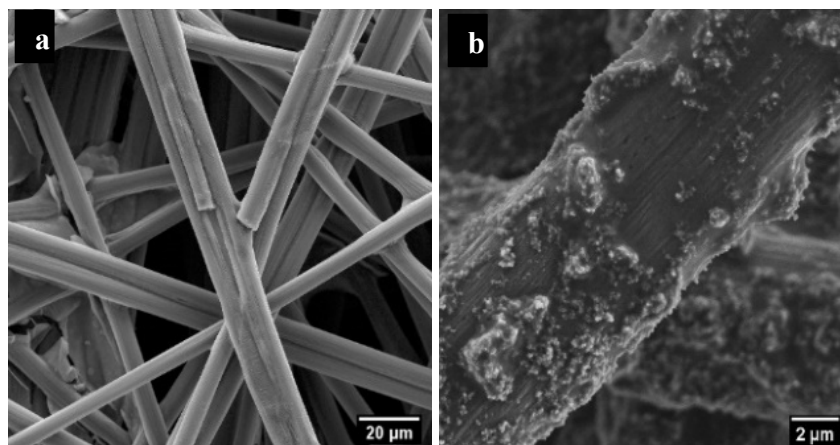


Fig. 2 SEM images of (a) Carbon paper, (b) CuO-C coated carbon paper

### E. Electrochemical Test

The electrocatalytic activity of the as-prepared electrocatalyst was evaluated by LSV using a three-electrode system in negative half-cell of VRFB. Catalyst layered carbon paper electrode (1 cm × 1 cm) as working electrode, Pt wire as a counter electrode, and Ag/AgCl electrode as reference electrode are used in this study. LSV tests were performed on Potentiostat (Make: Metrohm, Model: Autolab M204).

## III. RESULTS AND DISCUSSION

### A. Characterization

Fig. 2 shows the Scanning Electron Microscope images of the developed electrocatalyst. Fig. 2 (a) is the image of carbon paper support; Fig. 2 (b) is the image of electrocatalyst coated on carbon paper. It is apparent that the developed electrocatalyst coating results in some rough surface over smooth fibers of carbon paper.

Physical characterization of C, CuO and CuO-C electrocatalyst performed by XRD (Fig. 3) and the spectrum

obtained are in good agreement with the standard peaks of the materials that were mixed. The peaks at  $2\theta = 24.6^\circ$  (002) and  $43.3^\circ$  (101) are associated to carbon materials. The characteristic peaks at  $2\theta = 29.62^\circ$  (110),  $36.6^\circ$  (002),  $38.9^\circ$  (111),  $42.5^\circ$  (111) and  $61.6^\circ$  (113) are associated to CuO. The analysis of spectrum shows CuO-C is partially crystalline which can lead to high electrocatalytic activity [4].

Fig. 4 shows the FTIR spectrum of C, CuO and CuO-C electrocatalyst powder. The synthesized electrocatalyst has all the characteristic peaks of the mixed materials. The peaks at  $3425\text{ cm}^{-1}$  and  $3439\text{ cm}^{-1}$  represent the vibration of the -OH group and peaks at  $1630\text{ cm}^{-1}$  and  $1015\text{ cm}^{-1}$  represent the H-O-H stretching which may be mapped to surface absorbed water molecules. The -C-H<sub>2</sub> and -CH<sub>3</sub> stretching observed at  $2924\text{ cm}^{-1}$  signifies presence of carbon. Peak at  $1232\text{ cm}^{-1}$  confirms the present of CF<sub>2</sub> associated with nafion binder [5]. One sharp peak was observed at  $613\text{ cm}^{-1}$  in CuO spectrum which shows the CuO bond formation and peak at  $639\text{ cm}^{-1}$  rules out the presence of any other phase (Cu<sub>2</sub>O) [6]. Peak at  $540\text{ cm}^{-1}$  is

associated to Cu-O stretching vibrations.

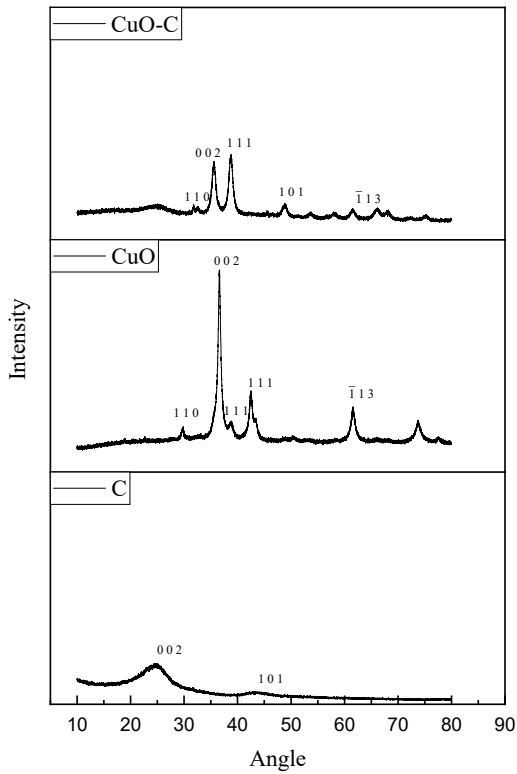


Fig. 3 XRD diffractogram of Carbon (C), CuO and CuO-C

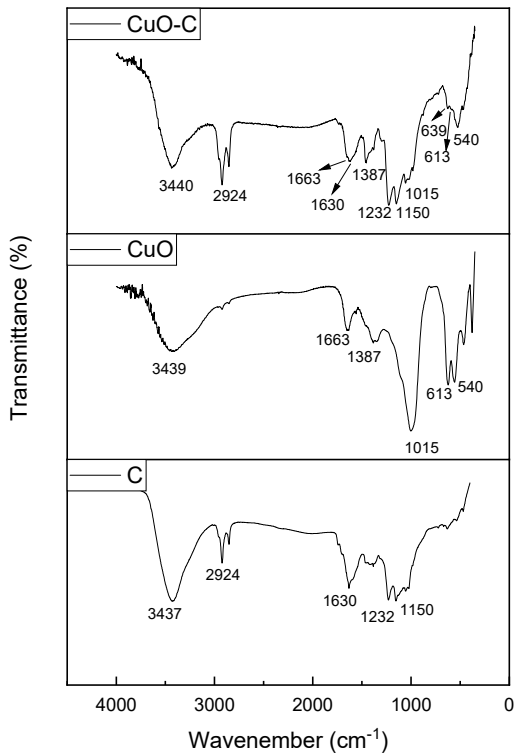


Fig. 4 FTIR spectrum of Carbon (C), CuO and CuO-C

*B. Linear Sweep Voltammetry test*

Linear sweep voltammograms CuO-C and CP electrodes are obtained for oxidation and reduction and shown in Figs. 5 and 6, respectively. The 1M  $V^{2+}$  in 3M  $H_2SO_4$  is used as an electrolyte and the potential range for LSV was from -0.5 V to 0.1 V vs. the Ag/AgCl reference electrode. The developed CuO-C has given the enhanced current density compared to CP as apparent in both of the voltammograms, which leads us to the conclusion that the system is having good electro-kinetic activity.

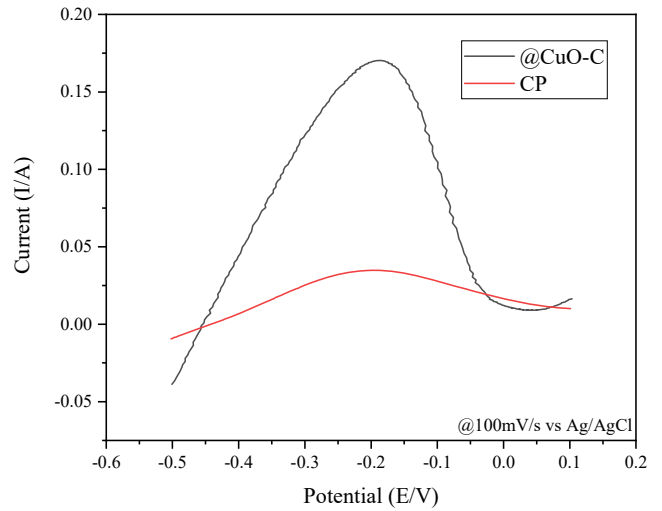


Fig. 5 LSV of CuO-C and CP in negative half-cell of VRFB for  $V^{2+}$  to  $V^{3+}$

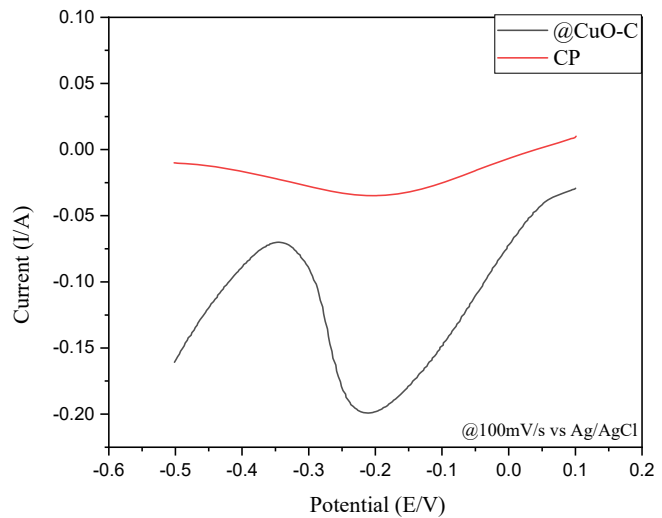


Fig. 6 LSV of CuO-C and CP in anodic half-cell of VRFB for  $V^{3+}$  to  $V^{2+}$

The data represented in Fig. 5 were further subjected to Tafel analysis. The Tafel slope for CuO-C electrode is 14 mV while the same for CP electrode is 63 mV in negative half-cell of VRFB shown in Fig. 7. It implies that the reaction kinetics for the VRFB system increased significantly [7].

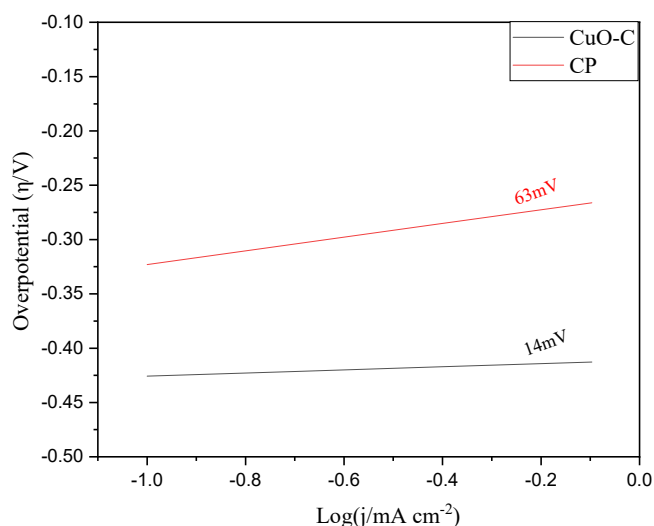


Fig. 7 Tafel plots

Further, the electrochemical active surface area (ECSA) is investigated for CuO-C and CP to obtain the insights of the electrodes [8]. The estimation of ECSA was carried utilizing Randles-Sevcik equation (4) for the quasi-reversible system shown in Fig. 7.

$$I_p = 2.99 \times 10^5 n(\alpha n)^{\frac{1}{2}} \times A D_o^{\frac{1}{2}} C_o v^{\frac{1}{2}} \quad (4)$$

where  $I_p$  = peak current (Amp),  $n$  = number of electrons transferred,  $\alpha$  = transfer coefficient (0.5),  $A$  = ECSA ( $\text{cm}^2$ ),  $D_o$  = Diffusion coefficient ( $\text{cm}^2\text{s}^{-1}$ ) [9],  $C_o$  = initial concentration of  $\text{V}^{2+}$  ( $\text{mol cm}^{-3}$ ).

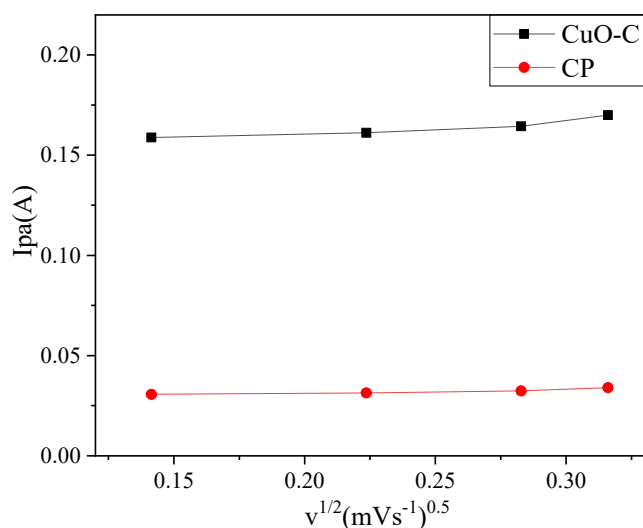


Fig. 8 Peak current vs. scan rate (Oxidation)

The slope of  $I_p$  vs. scan rate plots from Fig. 8 was used to calculate ECSA. An improved ECSA value is observed for CuO-C electrode which is  $8.8 \text{ cm}^2$  while the same for CP is  $2.6 \text{ cm}^2$ . This indicates that CuO-C has more surface area available for the transfer of electrons and having a high number of active sites than CP electrode.

The turnover frequency (TOF) was calculated using (5) [10] for LSV data of each electrode in  $1\text{M V}^{2+}$  in  $3\text{M H}_2\text{SO}_4$ .

$$TOF = \frac{I}{FN} \quad (5)$$

where  $F$  = Faraday constant ( $96485 \text{ C/mol}$ ),  $N$  = the number of active sites(mol),  $I$  = Current (A).

The number of active sites were determined by using (6) as this process is for one electron transfer. The total charge corresponding to CuO and CP was measured using both of the LSV curves (Oxidation and Reduction) in  $1\text{M V}^{2+}$  in  $3\text{M H}_2\text{SO}_4$  electrolyte at  $100 \text{ mV/s}$  scan rate.

$$N = \int_{V_1}^{V_2} I \Delta V / 2vF \quad (6)$$

where  $V$  = scan rate (mV/s),  $\Delta V$  = Potential window.

The number of active sites for CuO-C and CP electrodes are  $5.22 \times 10^{-6}$  and  $1.17 \times 10^{-6}$  moles respectively. The TOF values calculated for CuO-C and CP electrodes are  $0.335 \text{ s}^{-1}$  and  $0.300 \text{ s}^{-1}$  respectively at  $-0.2\text{V}$  potential. The CuO-C displays fivefold more active sites and higher TOF than CP, which suggests the improved reaction kinetics for the associated electrochemical reaction in negative half-cell of VRFB.

#### IV. CONCLUSIONS

The CuO was successfully synthesized utilizing microreactor. The developed CuO-C is showing all the characteristics of the mixed materials and it is validated through the XRD, FTIR and SEM results. The electrocatalyst enhanced electrochemical activity in the negative half-cell of VRFB. The higher current density reflects a reduction in charge transfer resistances for the anodic reaction. The tafel slope for the developed electrode shows the high electrocatalytic activity of CuO-C. the Higher ECSA, number of active sites and TOF values also suggest the improved kinetics of anodic reaction in VRFB. It can be concluded that the developed CuO-C is suitable for negative half-cell of VRFB.

#### REFERENCES

- [1] M.M. Seepana, S. Samudrala, P. V Suresh, R. Vooradi, "Unit Cell Modelling and Simulation of All Vanadium Redox Flow Battery," 13 (2018).
- [2] N. Roznyatovskaya, J. Noack, K. Pinkwart, J. Tübke, "Aspects of electron transfer processes in vanadium redox-flow batteries," Curr. Opin. Electrochem. 19 (2020) 42–48.
- [3] L. Xu, C. Srinivasakannan, J. Peng, L. Zhang, D. Zhang, "Synthesis of Cu-CuO nanocomposite in microreactor and its application to photocatalytic degradation," J. Alloys Compd. 695 (2017) 263–269.
- [4] W.-J. Jiang, S. Niu, T. Tang, Q.-H. Zhang, X.-Z. Liu, Y. Zhang, Y.-Y. Chen, J.-H. Li, L. Gu, L.-J. Wan, J.-S. Hu, "Crystallinity-Modulated Electrocatalytic Activity of a Nickel (II) Borate Thin Layer on Ni 3 B for Efficient Water Oxidation," Angew. Chemie. 129 (2017) 6672–6677.
- [5] I.U. Khan, M. Mohan Seepana, K.S. Rajmohan, J. Pandey, "Electrochemical activity of tungsten oxide doped carbon (WO<sub>3</sub>/C) catalyst for hydroquinone/benzoquinone redox flow battery," Mater. Lett. (2023) 134355.
- [6] A.B. Bodade, M.A. Taiwade, G.N. Chaudhari, "Bioelectrode based chitosan-nano copper oxide for application to lipase biosensor," J. Appl. Pharm. Res. (JAPTRonline). 5 (2017) 30–39.
- [7] D.S. Cheng, E. Hollax, "The Influence of Thallium on the Redox Reaction  $\text{Cr}^{3+}/\text{Cr}^{2+}$ ," J. Electrochem. Soc. 132 (1985) 269–273.

- [8] S. Mousavihashemi, S. Murcia-López, M.A. Rodríguez-Olguin, H. Gardeniers, T. Andreu, J.R. Morante, A. Susarrey Arce, C. Flox, "Overcoming Voltage Losses in Vanadium Redox Flow Batteries Using WO<sub>3</sub> as a Positive Electrode," *ChemCatChem*. 14 (2022).
- [9] G. Orijji, Y. Katayama, T. Miura, "Investigations on V(IV)/V(V) and V(II)/V(III) redox reactions by various electrochemical methods," *J. Power Sources*. (2005).
- [10] Z. Jin, P. Li, X. Huang, G. Zeng, Y. Jin, "electrocatalyst for hydrogen evolution †," (2014) 18593–18599.